Development of a Beam Dynamic Design Code for Proton Travelling Wave Linacs

YANG Yufei, WAN Xinmiao, PU Xuejiang, REN Zhiqian, LIN Pengtai, LI Zhihui†

(*The Key Laboratory of Radiation Physics and Technology of Ministry of Education, Institute of Nuclear Science and Technology, Sichuan University, Chengdu 610065, China*)

Abstract: The field of proton accelerators research is experiencing a surge of interest as proton beams find wide applications in areas like cancer therapy, industrial applications, and scientific researches. The recent advancements in high gradient radio frequency standing wave and travelling wave ion accelerating structures, reaching frequencies of several GHz in the past few years, have paved the way for compact linear ion accelerators with high gradients. Compared with the abundant design code for standing wave ion linacs, the design code for travelling wave structure is very limited. We developed a new type of particle dynamics tracking (*PDT*) code, which can be used in beam dynamics design for both standing wave and travelling wave structures based on the electromagnetic field distribution of the unit cell. The benchmark with the widely used commercial linac beam dynamics simulation code *TraceWin* shows its accuracies both in energy gain and envelopes are good. The code has been applied in the beam dynamics design of a low current backward travelling wave proton linac, which operates at RF frequency of 2.856 GHz and working at 5π/6 mode. The linac spans a total length of approximately 3 m, comprising 10 tanks and 10 PMQs (Permanent Magnet Quadrupoles). It operates with a 30 MV/m accelerating gradient, characterized by full transmission and minimal emittance growth.

Keywords: Proton beam; Travelling wave; Particle dynamics; Beam matching; Linac

1 Introduction

Way back in the beginning of the last century, the proton accelerator has been put forward and operated successfully, and various types of accelerators have been clearly thriving ever since. The accelerated particle beams have a wide range of applications and prospects in many areas such as nuclear physics [1], materials science, space exploration and especially in radiation treatment [2-3]. In recent years, proton and heavy ion radiotherapy have seen rapid development worldwide. At the time of writing, January 2023, there are around 120 particle therapy facilities in operation and most of them are based on cyclotrons and synchrotrons [4].

The frequency of proton linear accelerators (linacs) are typically 200-400 MHz, with a low acceleration gradient and large volume, coupled with large-scale investments. This is one of the limiting factors that limits proton therapy from becoming the standard of broader cancer care at present. High accelerating gradient ion linacs have become feasible solutions with S-band frequencies, which also provides a new idea for the application of proton linac. A research group designed the LIBO (LInac BOoster), a side-coupled Linac that works at 3 GHz and whose effective accelerating gradient can reach 28.5 MV/m, can be used downstream of a linac or a cyclotron, to boost the low energy of proton beam from about 60 MeV to 200 MeV or more[5-6]. ACCIL is a compact ultra-high gradient coupled cavity linac (CCL) acceleration structure that operates at 2856 MHz and can accelerate up to 50 MV/m. Its RF parameters degrade dramatically for

Received date：yyyy-mm-dd; **Revised date**：yyyy-mm-dd

Foundation item：National Natural Science Foundation of China (11375122 and 11875197)

Biography：YANG Yufei(2000-), Chengdu, Sichuan province, postgruaduate, Working on physics of particle accelerator; E-mail: yyf6935@163.com

†**Corresponding author**：LI Zhihui, E-mail: lizhihui@scu.edu.cn

structures with β<0.7 [7-8]. The TULIP project is dedicated to the development of a compact proton linac. A new backward travelling waveguide (BTW) RF structure with a high gradient is designed, which can meet the accelerating gradient of 50 MV/m. The low shunt impedance caused by low-β CCL structure is solved by adding external disc coupling holes for magnetic coupling. In order to achieve low peak electric field and high shunt impedance with lower β, the article [9] proposed to synchronize beam with the -1 harmonic wave, which will prolong the acceleration period and increase the shunt impedance without significantly increasing the peak field.

While *TraceWin* is capable of simulating beam dynamics through fixed standing wave structures, it may not provide extensive design support for travelling wave RF structures [10]. In the literature [11-12], a structure optimization by polynomial fitting (*SOPF*) for standing wave structures is compiled, which is a multi-objective optimization algorithm. The frequency sensitive values were obtained by the scanning points, and a complete database was established by polynomial fitting according to the analysis results, and the relevant parameters were finally determined. There are also codes that can track particles through travelling wave structures, such as *RF-Track* [13-14], which can be used to maximize the transmission effect as well as validate the lattice design.

Compared with the abundant available design tools for standing wave proton linac, the design tool for tracking protons through travelling wave structures is relatively hard to find. Since the electromagnetic structure design and particle dynamics design are closely related, it is important to find a starting point. It is urgently needed to compile the particle dynamics tracking (*PDT*) code of our own, which can meet the needs, including precise tracking of single-particle and beams of protons, as well as automatically optimization tuning of cavity structural parameters. Moreover, we can add functions to the system according to our specific requirements flexibly, rather than using a stereotyped black-box tool. It can perform dynamics simulation for not only a single acceleration structure, but also for different situations under different types of acceleration structures, modes and frequencies, etc. At the same time, a proton linac based on high gradient backward travelling wave is designed by using this new tracking code. This linac requires minimum RF design input (cell optimization results), and its application on the 100 MeV BTW proton linac beam dynamics simulation is presented.

Except the introduction, the paper is divided into three parts: Firstly, the dynamic equations and algorithms outline used in *PDT* code are introduced in detail, including the function expression of travelling wave field in periodically loaded waveguide and its establishment with the help of CST, longitudinal and transverse particle tracking and beam matching, as well as the automatic tuning of RF waveguide structure. In the second part, we make a benchmark of *PDT* code with *TraceWin*, and the simulation results are in good agreement, which verifies the feasibility of *PDT*. The third part is to simply design a multi-tanks linac with an acceleration gradient of 30 MV/m to boost the energy of 30 MeV up to 102.9 MeV in the case of protons, with a RF frequency of 2.856 GHz and phase advance of 5π/6. A preliminary dynamics study has been carried out using *PDT*.

2 Particle dynamics tracking and optimization by PDT code

To study the dynamic process of protons in the travelling wave accelerating structures, it is necessary to establish a physical model of the electromagnetic field first. The typical modeling method is to build a three-dimensional cavity model, and the widespread availability of commonly used simulation software such as SUPERFISH [15] and CST studio suite [16] makes it feasible to extend the use of these programs to travelling wave structures.

The whole solving process is mainly divided into two modules. The simulation model integrative framework is proposed as in Fig.1. The first step is to make full use of automated MATLAB [17] and CST co-simulation to track the dynamics of a single particle in the longitudinal direction and finish the main accelerating cavity design (RF structure tunning). The linac typically comprises accelerating tanks, and each tank is composed of multiple cells of equal length. The particle velocity, β_z, within each tank remains almost constant and changes very little, and the corresponding cell length change is less than 0.1 mm. However, the β_z value varies significantly between tanks, and this cannot be disregarded. As a result, the length of the cells in the adjacent tank needs to be adjusted based on the β_z value. We utilize

CST to model and tune the single cell with periodic condition calculating the electromagnetic field on the central axis. Structure parameters such as iris aperture radius, cavity radius and the radial distance of coupling holes, etc. are calculated by CST optimizer combined with the required RF characteristics and cell length. After calculating the electric field distribution of the unit cell in first tank with specific geometric parameters, dynamics tracking of the particles through the tank is carried out in MATLAB. Compute the structure parameters of the unit cell in the next tank, such as the cell length, tube length even the optimal cell numbers through the particle output state parameters in end of last tank, and take them as new input parameters of CST simulation. This cycle continues until the particles are accelerated to the specified energy.

On account of the multi-parameter optimization of the unit cell in each tank must be carried out strictly step by step manually adjusting, making the whole process very slow. The tuning work and stored procedure involved can be very complex and time-consuming. In order to enable the dynamic invocation, automating RF structure geometric parameters, the code has added this module to create appropriate wires to enable communication between *PDT* and CST, for speeding up the design process.

Into the second module, beam dynamic design is carried out. Including transverse focusing of FODO-like lattice approximate matching problem, and finally obtaining the optimal Twiss parameters and lens gradients to achieve maximum transmission. As well as longitudinal and transverse multi-particle tracking.

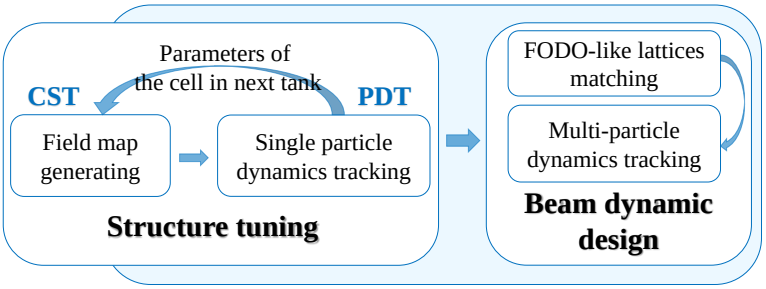

Fig.1 (color online) The Simplified scheme of *PDT* code architecture

2.1 Travelling wave field in a periodically loaded waveguide

By CST, the longitudinal field of travelling wave along travelling wave accelerating structure at a certain time can be calculated, and then the longitudinal and transverse fields at any other time are represented by transformation methods presented in the following sections, which avoids the heavy calculation process and greatly reduces the amount of calculation.

The total field of the lowest order passband of TM01 mode in periodically loaded waveguide can be expressed as the sum of all harmonic fields [18-19], and simplified as:

$$E_z(r,z,t) = A_z(r,z)e^{j(\omega t-\phi_z(r,z))} \tag{1}$$

The total field is simplified into the exponential form of a complex variable function, that is, the function of the amplitude A_z and phase ϕ_z of the electric field. The field satisfies Maxwell's equations and boundary conditions at any time. By obtaining the field along the cavity axis at a specific time t_0, we can determine the longitudinal field of the traveling wave at any other time. For a multi-cell structure, according to Floquet's theorem, the fields of the cells differ only by a constant complex factor, which is denoted as the periodic phase shift σ. Then, we can obtain the field along the multi-cell periodic loaded waveguide at any time based on the amplitude A_z and phase $\varphi_z(t_0) = \omega t_0 - \phi_z$ function obtained from this single cell field calculation. And the field of cell n with equal length l appears as follows:

$$E_z(z+nl, t+t_0) = A_z e^{j(n\sigma+\omega t-\varphi_z(t_0))} \tag{2}$$

where E_z, A_z and φ_z are all functions that change with z. In the case of a proton machine, the constant gradient mode is commonly employed, where the cell length is maintained constant within a short section of the waveguide for a compromise between simple fabrication and a little cost of a phase slippage and efficiency loss [20]. There is coupling

effect between the transverse field and the longitudinal field in the passive case according to Maxwell's equations and axial symmetry [21], the transverse electric and magnetic fields under the paraxial approximation can be represented by the longitudinal electric field:

$$\begin{cases} E_r = -\dfrac{\partial E_z}{\partial z}\dfrac{r}{2} = -\dfrac{r}{2}\left[\dfrac{dA_z}{dz}e^{j(n\sigma+\omega t-\varphi_z(t_0))} - j\dfrac{d\varphi_z}{dz}A_z e^{j(n\sigma+\omega t-\varphi_z(t_0))}\right] \\ B_\theta = \dfrac{r}{2c^2}\dfrac{\partial E_z}{\partial t} = j\dfrac{r\omega}{2c^2}A_z e^{j(n\sigma+\omega t-\varphi_z(t_0))} \end{cases} \tag{3}$$

As a result, according to the longitudinal electric field at a certain time within a unit cell, the electric field value and angular value of magnetic field at any position near the axis at any time in the acceleration gap can be obtained. Based on the established travelling wave field, we can further analyze and discuss the transverse and longitudinal dynamic equations of particles, and solve the bunched beam problem in periodic focusing channel.

2.2 Longitudinal dynamic equations and the algorithm

The velocity v_z of the proton passing through the cavity will change with the longitudinal distance z. Let the relative phase of the particle entering the cavity be θ_0 and the phase of the time component can be expressed as the position component α_z. And the voltage $V(\theta_0)$ felt by the particle through the whole cavity is the integral of the longitudinal electric field along the path. Obviously, we can find a θ_i that $V(\theta_i)$ reaches a maximum, and particles gain greatest acceleration with this incident phase also called synchronize 0° phase. However, in order to accelerate the particles stably and considering the particles capture efficiency, it's necessary to choose a synchronous phase for achieving a compromise between less particle loss and higher acceleration efficiency.

According to the conservation of energy, when the acceleration structure is in TM01 mode, only the longitudinal electric field contributes to the energy gain, and the longitudinal motion equations can be expressed as:

$$\begin{cases} \dfrac{d\gamma}{dz} = \dfrac{qA_z}{m_0c^2}\cos(\alpha_z - \varphi_z + \theta_0) \\ \dfrac{d\omega t}{dz} = \dfrac{\omega}{c}\cdot\dfrac{1}{\beta_z} \end{cases} \tag{4}$$

where the independent variable is z, θ_0 is the initial input phase. In order to achieve the maximum acceleration efficiency, it is crucial for the speed of the travelling wave in the accelerating cavity to match the speed of the particles. This relationship is described in detail in section 4. When the number of particles is increased and the initial phase difference and energy difference are within a certain range relative to the reference particle, each particle can be tracked and positioned to obtain longitudinal phase space diagram of the particles.

The amplitude and phase of the electric field of unit cell were derived from CST simulation and then imported into MATLAB for further analysis. The leapfrog algorithm was employed to solve the longitudinal dynamic differential equations of the particles, with the appropriate step threshold selected, to calculate and record the longitudinal velocity state quantity β_z and the phase state ϕ_z of particles simultaneously. Leapfrog algorithm is fast and accurate enough. And cyclic optimization algorithm is used to calculate the synchronize 0° phase θ_i, that is, the incident phase when the particle gets the maximum energy gain.

After tracking and recording the state quantities of the longitudinal motion of a single particle, the tracking calculation for multi-particles is performed based on the incident condition determined by the reference particle, which corresponds to the one with the optimal incident phase θ_i that we previously sought.

2.3 Transverse dynamic equations and algorithm

The transmission efficiency is closely related to the transverse emittance of the beam. In the context of a linac accelerating particles longitudinally, it is important to consider the impact of the cavity on the transverse dynamics of the

particles. The electromagnetic field can induce defocusing effects on the particles in the transverse direction, potentially leading to an increase in the particle's radial distance from the ideal beam path. Excessive radial distances can result in particle loss and decreased transmission efficiency. To study the transverse dynamics of a single particle, the transverse dynamic equations are analyzed. For a bunched beam consisting of thousands of particles, the envelope equation is considered to understand the collective behavior of the beam. Then using *PDT* code to simulate the transverse dynamics of the tracking particles with the increase of energy, and to match FODO-like lattice periodic beam channel.

Analyze the transverse force on the individual particles, and substitute the radial electric field and angular magnetic field formulas derived in formula (3). The dynamic equations can be obtained:

$$\begin{cases} \dfrac{dp_r}{dz} = -\dfrac{q}{2v_z}\left(\dfrac{\partial E_z}{\partial z} + \dfrac{\beta_z}{c}\dfrac{\partial E_z}{\partial t}\right) r \\ \dfrac{dr}{dz} = \dfrac{p_r\sqrt{1-\beta_z^2}}{m_0 v_z} \\ p_z = \dfrac{m_0 v_z}{\sqrt{1-\beta_z^2}} \end{cases} \tag{5}$$

where $q = e = 1.6 \times 10^{-19}C$, the unit of p_r is $kg \cdot m/s$ and:

$$\begin{cases} \dfrac{\partial E_z}{\partial z} = \dfrac{dA_z}{dz}\cos\left(\phi_0 - \phi_z(z) + \omega t\right) + \dfrac{d\phi_z}{dz}\sin\left(\phi_0 - \phi_z(z) + \omega t\right) \\ \dfrac{\partial E_z}{\partial t} = -\omega\sin\left(\phi_0 - \phi_z(z) + \omega t\right) \end{cases} \tag{6}$$

According to the incompatibility theorem, in the process of acceleration longitudinally, the RF electric field presents the impact of defocusing to the beam transversely. To counteract this defocusing effect, external permanent magnetic-quadrupole lenses are needed. These lenses can be strategically placed to focus the beam and compensate for the defocusing caused by the RF electric field. By properly adjusting the strengths of these lenses, the beam can be kept in a tightly focused state, leading to improved transverse dynamics and reduced emittance growth. In the high-energy tank, the beam emittance is low enough that the FODO-like periodic structure can be adopted. However, it is important to note that in a proton Linac lattice, unlike a regular FODO lattice, the length of the accelerator structure grows proportionally to the relativistic beta of the accelerated particle.

The transverse motion of a single proton is generally measured by four-dimensional parameters, including two position states x, y and two momentum states P_x, P_y or velocity states v_x, v_y or by the inclination $x' = v_x/v_z = P_x/P_z$, $y' = v_y/v_z = P_y/P_z$. In addition, the Twiss parameter is generally used to describe the bunched beam envelope. The general formula for a phase space ellipse (an ellipse in the plane with axis x-x' and containing phase space particles for example) is as follows:

$$\left[\frac{x + (\alpha_x/\gamma_x)x'}{\sqrt{\varepsilon_x/\gamma_x}}\right]^2 + \left(\frac{x'}{\sqrt{\varepsilon_x\gamma_x}}\right)^2 = 1 \tag{7}$$

And the same is true in y-direction. Where γ, α, β are Twiss parameters or so-called Courant-Snyder parameters, neither of which are independent parameters, but together constitute Courant-Snyder conditions:$\gamma\beta - \alpha^2 = 1$.

The distribution modes of the beam particles in phase space are Gaussian and Kapchinskij-Vladimirskij (*KV*) distribution for typical numerical simulating. The more significant that need to be studied is the central and denser part of a beam while the outer parts of a beam with a very low density are usually not very important. The relation between the total emittance of n-dimensional uniform hyperellipsoid and rms emittance is that $\varepsilon_{total}=\varepsilon_{rms}(n+2)$. When $n=2$, the points in the four-dimensional ellipsoid are uniformly distributed on all its two-dimensional projections, which is also known as *KV* distribution [21]. When x and y planes are both considered transversely, the four variables (x, x', y, y') are considered to obey *KV* distribution in the four-dimensional space, then there is $\varepsilon_{total}=4\varepsilon_{rms}$:

$$\left[\frac{x+(\alpha_x/\gamma_x)x'}{\sqrt{\varepsilon_x/\gamma_x}}\right]^2+\left(\frac{x'}{\sqrt{\varepsilon_x\gamma_x}}\right)^2+\left[\frac{y+(\alpha_y/\gamma_y)y'}{\sqrt{\varepsilon_y/\gamma_y}}\right]^2+\left(\frac{y'}{\sqrt{\varepsilon_y\gamma_y}}\right)^2=1 \tag{8}$$

In the *PDT* code, under the given Twiss parameters and emittances within limits over two transverse directions, take a required number (the input particle quantity) of groups of uniformly distributed pseudo-random numbers in a certain range for three parameters Φ_1, Φ_2, $\Phi_3 \in [0,2\pi]$, which meet the condition:

$$(\cos\Phi_1\cdot\cos\Phi_2)^2+(\sin\Phi_1\cdot\cos\Phi_3)^2+(\cos\Phi_1\cdot\sin\Phi_2)^2+(\sin\Phi_1\cdot\sin\Phi_3)^2=1 \tag{9}$$

Then we can assign the values to the transverse state quantities (x, x', y, y') of particles:

$$\begin{cases}\dfrac{x+(\alpha_x/\gamma_x)x'}{\sqrt{\varepsilon_x/\gamma_x}}=\cos\ \Phi_1\cdot\cos\ \Phi_2\\ \dfrac{y+(\alpha_y/\gamma_y)y'}{\sqrt{\varepsilon_y/\gamma_y}}=\cos\ \Phi_1\cdot\sin\ \Phi_2\\ \dfrac{x'}{\sqrt{\varepsilon_x\gamma_x}}=\sin\ \Phi_1\cdot\cos\ \Phi_3\\ \dfrac{y'}{\sqrt{\varepsilon_y\gamma_y}}=\sin\ \Phi_1\cdot\sin\ \Phi_3\end{cases} \tag{10}$$

The input emittance is the single plane RMS emittance $\varepsilon_{n.rms}$, which need to be converted into unnormalized emittance $\varepsilon_{rms}=\varepsilon_{n.rms}/\beta_0\gamma_0$ and then to the total emittance of hyperellipsoid $\varepsilon_{total}=4\varepsilon_{rms}$. According to the transverse dynamic formulas (5-6), calculate and track the motion state x, x', y, y' of each particle with *PDT* code, of which we use difference method to calculate the partial derivative of electric field.

After tracking a bunch of particles with typical input parameters for a test, it is observed that the particles pass through a continuous periodic RF structure with an accelerating gradient of 30 MV/m. The resulting phase space distribution diagram, shown in Figure 2, indicates that the bunches have diverged noticeably. This divergence is evident in the x-x' phase space as larger displacements and velocity divergences, while in the y-y' phase space, the beam transitions from a convergent state with a negative parameter α to a divergent state with a positive α.

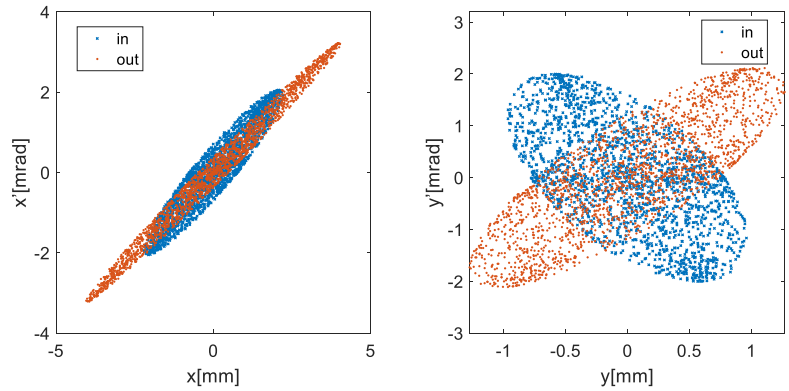

Fig.2 (color online) The distribution of the particles in unnormalized transverse phase-space at the beginning (blue) and at the end (red) of the acceleration

Excessive transverse drift distance will result in increased particle losses. To deal with it, it is essential to introduce elements with focusing capability. A FODO-like lattice is composed of two acceleration tanks and two PMQs in such structure in alternating arrangement, where each tank consists of several identical RF structure cells. To find the matching point of the Twiss parameters to the gradient of the PMQs, a process known as matching, it is necessary to ensure that the beam's transverse properties align with the focusing strength provided by the PMQs.

The linearization of the change in transverse position and velocity inclination of the particle between the two positions can be expressed by a 2×2 transfer matrix M. Then the transfer matrix of the accelerating cavity can be

obtained in this way. Assume that $P_x = x' \cdot \beta\gamma$, then we have the normalized motion state which is:

$$\begin{bmatrix} x_2 \\ P_{x2} \end{bmatrix} = \begin{bmatrix} 1 & 0 \\ 0 & \frac{1}{\beta_2\gamma_2} \end{bmatrix}^{-1} \cdot M \cdot \begin{bmatrix} 1 & 0 \\ 0 & \frac{1}{\beta_1\gamma_1} \end{bmatrix} \cdot \begin{bmatrix} x_1 \\ P_{x1} \end{bmatrix} = M^* \cdot \begin{bmatrix} x_1 \\ P_{x1} \end{bmatrix} \tag{11}$$

For periodic FODO structure, its transfer matrix can be expressed by Twiss parameter:

$$M^* = \begin{bmatrix} \cos\mu + \alpha\sin\mu & \beta\sin\mu \\ -\gamma\sin\mu & \cos\mu - \alpha\sin\mu \end{bmatrix}, |M^*| = 1 \tag{12}$$

In the case of calculating the transfer matrices for the accelerating cavity, the calculation is based on the state quantity of the particles. These transfer matrices are independent of the motion of individual particles and the presence of the PMQs. Instead, they solely depend on the structure of the accelerating cavity. Therefore, once the structure of each tank is determined, the corresponding transmission matrix, denoted as *M**, can be calculated using equation (12).

Regarding the PMQs, its characteristics dictate that it cannot simultaneously focus or defocus in both the *x* and *y* directions. The transfer matrix associated with the PMQs differ between the two transverse directions:

$$\mathrm{R}_{\mathrm{focus}} = \begin{bmatrix} \cos\sqrt{K}l & \frac{\sin\sqrt{K}l}{\sqrt{K}} \\ -\sqrt{K}\sin\sqrt{K}l & \cos\sqrt{K}l \end{bmatrix}, \mathrm{R}_{\mathrm{defocus}} = \begin{bmatrix} \cosh\sqrt{K}l & \frac{\sinh\sqrt{K}l}{\sqrt{K}} \\ \sqrt{K}\sinh\sqrt{K}l & \cosh\sqrt{K}l \end{bmatrix} \tag{13}$$

where $K = qG/mc\beta\gamma = q(B/r)/mc\beta\gamma$, G is the gradient of the quadrupole lens (in *T*/*m*), B is magnetic field intensity at pole tips, l is the length of the lens.

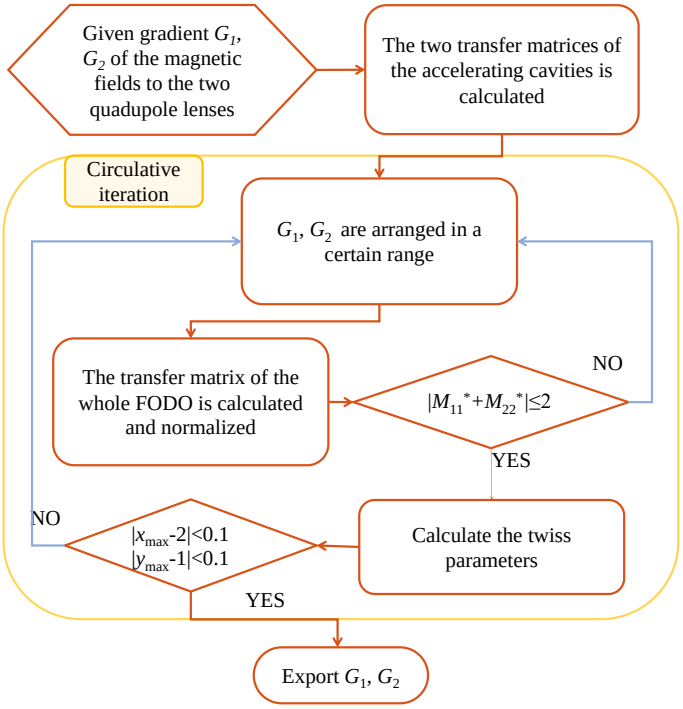

Fig.3 (color online) Solving procedure to match the beam in a FODO-like lattice

Fig.3 shows the matching process. A FODO-like lattice transfer matrix is changed by adjusting the parameters G_1 and G_2 of two quadrupole lenses with fixed parameters of the acceleration cavities. The Twiss parameters, for depicting the envelope of the phase-space ellipse, obtained by matching the import beam to export in this lattice after normalization. The next steps are calculated after un-normalization.

In the optimization process, numerically, there will be such a situation that the trace of the matrix $|M_{11}^* + M_{22}^*| > 2$, in which the matching solution or a matched beam condition does not exist. Hence, there's need to adjust the gradients G_1 and G_2 of the two quadrupoles lens so that the x direction meets $|M_{11}^* + M_{22}^*| \leq 2$, and the same is true in y direction. The code seeks results automatically after the end of the longitudinal dynamics design, allowing determination of optimal

Twiss parameters of the phase space ellipse and gradients of the magnetic-quadrupole lens which leads to best transmission. Ultimately, in a testing FODO-like lattice structure, the normalized envelope of phase-space ellipse in the two directions is shown in Fig.4. It reveals that the normalized ellipse almost matches perfectly.

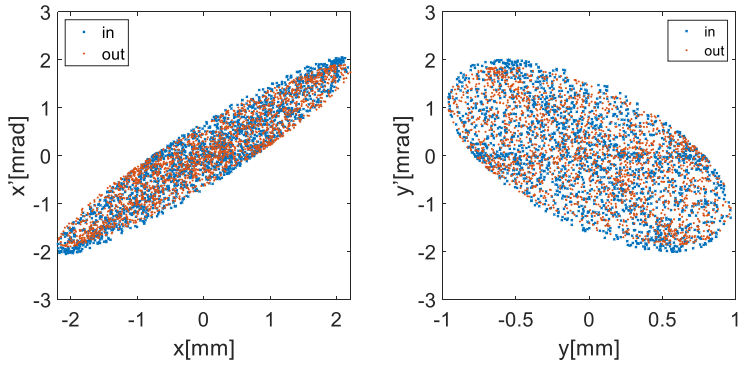

Fig.4 (color online) The distribution of the particles in normalized transverse phase-space at the beginning (blue) and at the end (red) of an optimal matched FODO-like lattice solved by *PDT*

3 Benchmark

Here a coupled cavity linac (CCL) structure is considered for the benchmark against *PDT* and *Tracewin*, which demands as an input the standing wave field map. Nevertheless, standing wave is actually a special form of travelling wave. CST is used to generate the electromagnetic field map of CCL structure for a single cell.

In this scenario, a group of 10,000 protons with an incident kinetic energy of 85.8 MeV undergo transportation through a FODO lattice. The lattice consists of two 7-cell CCL accelerating tanks responsible for boosting energy and two PMQs for focusing. The system operates at a frequency of 2.97863 GHz, and the dimensions of the acceleration structure can be found in Table 1. Given the same particle incident phase 117 deg and initial emittance of 0.3978 π·mm·mrad, the optimal matching values are obtained respectively by automatic optimization. The results demonstrate reliability and accuracy in terms of kinetic energy growth, transverse emittance, and the gradients of the PMQs.

Table 1 The specific parameters of benchmark

	Emittance (Norm.) [π·mm·mrad]	Output energy [MeV]	PMQs gradients [T/m]	Acceleration structure length [m]			
PDT	0.398	89.506	445/445	CCL cell	PMQs	Drift	Active/Total
TraceWin	0.400	89.457	446/447	0.0202	0.02	0.01	0.2828/0.3622

The phase space distribution of particles, both in terms of envelope and Twiss parameters, exhibits a good fit with the results obtained from both PDT and *TraceWin*, and is shown in Fig.5. Furthermore, the variation of the final energy of the particles with the input phase also exhibits a high level of agreement, with an error within 0.02%. These findings showcase the accuracy and effectiveness of the *PDT* code used in the study.

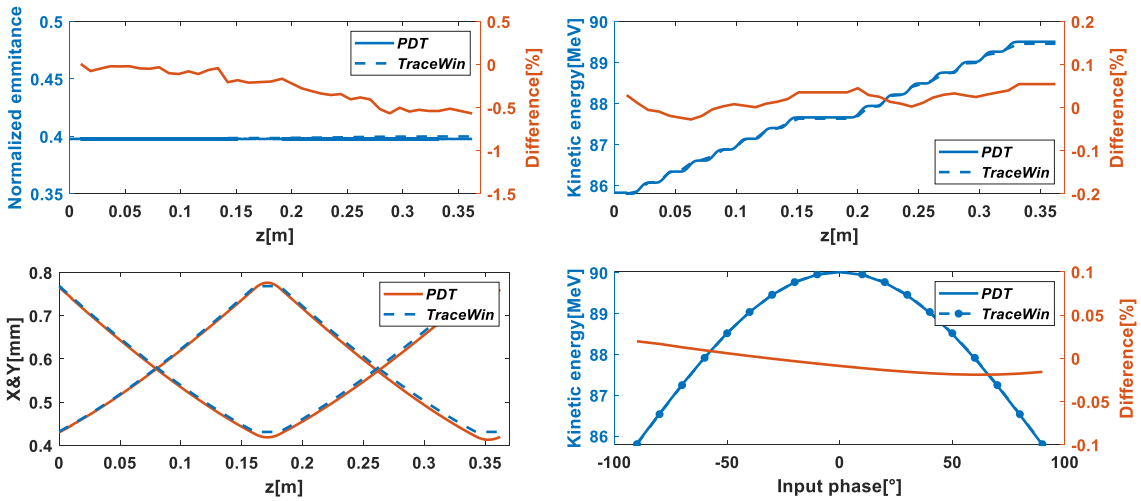

Fig.5 (color online) Normalized emittance and envelope of the phase-space ellipse (left)

Kinetic energy grows with accelerating and final energy varies with input phase (right)

4 Dynamics simulation of a 30MeV-100MeV multi-tanks BTW linac

The CS-30 cyclotron, in operation by the Institute of Nuclear Science and Technology of Sichuan University, can accelerate protons, deuterons and α particles, the energy of extracted proton beams is about 30 MeV [22], is a good candidate for high gradient acceleration structure test. What we expect is to take proton beams to a higher energy to make it more serviceable in wider applications. The author has designed a S-band side-coupled cavity linac (SCL) for re-accelerating proton beam from 26 MeV up to 120 MeV, its shunt impedance ranged from 22.5 to 59.8 MΩ/m, and the designed acceleration gradient is about 13 MV/m, however suffering hardship of the tuning of the cells [23]. The BTW exhibits superior performance in terms of shorter filling time, higher TT factor, sharper nose angle in the nose region, and approximate values of ZTT [24-25], contributes to make feasible a compact S-band BTW proton linac.

Protons are decided to be injected into a BTW linac with an acceleration gradient of 30 MV/m, operating at f = 2.856*GHz*. The linac is composed of 10 accelerating tanks, and each tank consists of multiple BTW cells of equal length. In the process of acceleration, there can be transverse divergence of particles due to the RF fields, and *PDT* code optimization algorithm is used to make transversely beam matching.

4.1 BTW structural parameters tuning

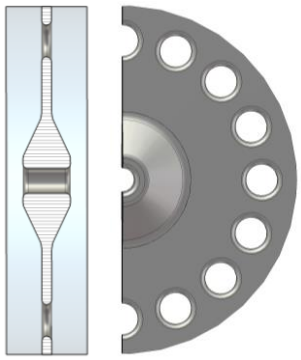

Fig.6 (color online) Model diagram of BTW accelerating structure

The geometry of the regular BTW cell structure is depicted in Fig.6. It is recognized that the thickness of the iris influences the shunt impedance and mechanical resistance of the structure remarkably. We can adjust the wave velocity by varying the cell length. In addition, group velocity is related to the radius of coupling holes. The group velocity is changed by changing the size of the coupling holes for travelling wave structure, which is located far away from the beam

axis, and it is reasonable to assume that the field along axis is unaffected by the size of coupling holes. The RF frequency is related to the cell cavity diameter and the radial distance of coupling holes. Fig.7 illustrates the longitudinal field amplitude and phase of a two-cell constant gradient structure constructed from single cell calculation results.

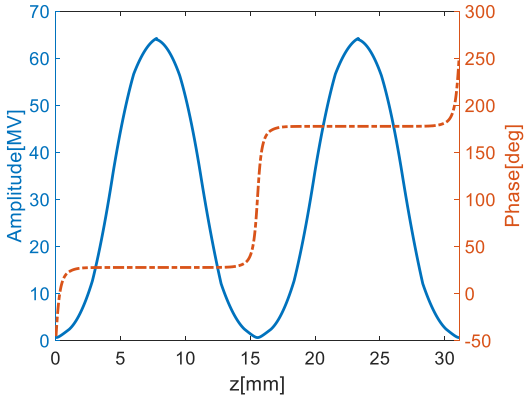

Fig.7 (color online) The amplitude and phase of the electric field of the adjacent units under periodic cells

The relation between the cell length L_{cell} and the phase velocity β_p of the BTW cell, the phase advance σ and frequency f of travelling wave is as follows:

$$L_{cell} = \frac{\sigma \beta_p c}{2\pi f} \tag{14}$$

f=2.856GHz and σ=5π/6 of each cell are constant, the length L_{cell} has a linear relation with phase velocity β_p. The initial energy of the particle is 30 MeV, where we have particles initial velocity β_0=0.247. When the acceleration of first tank is finished, the particles enter the next cavity for acceleration with velocity increasing significantly. Therefore, the phase velocity of the travelling wave in the next tank should be increased accordingly to make the it consistent with the particle velocity as far as possible and follow the rule between β_p and β_0 in the meantime, so as to achieve the highest acceleration efficiency.

The transit-time factor (*TTF*) is the ratio of the actual energy gain in an acceleration cavity to the energy gain obtained by the specific dc field, and represents the acceleration efficiency of the cavity [21]:

$$TTF = \frac{\int_0^L A_{z,\,\mathrm{real}} \cos\left(\alpha_z - \varphi_z + \theta_0\right) dz}{\int_0^L A_{z,\,\mathrm{real}}\, dz} \tag{15}$$

The *TTF* value is affected by the initial velocity, incident phase, the number of cells in each tank and travelling wave phase velocity. The left figure in Fig.8 shows the change of the maximum *TTF* with the number of cells and phase velocity β_p of travelling wave and the parameters of the acceleration cavity change correspondingly with it, enable finding the optimal value for number of the cells in a tank. On the other hand, it is hoped that each tank contains as many cells as possible to make the particle energy reach 100 MeV as soon as possible. A compromise is considered to select 17 BTW cells in each tank.

When keeping the parameters of cavity constant, the ratio of the energy gain with respect to the maximum energy gain V/V_{max} of the reference particle in a tank varies with the particle initial velocity β_0 and the number of cells, as shown in the Fig.8 on the right. In the graph, it is observed that when the phase velocity of wave is constant β_p=0.257, the influence of the number of cells on the optimal incident velocity of particles is not significant. And the optimal incident velocity β_0=0.247 of particles in the first tank can be obtained, corresponding to the incident energy of 30 MeV. Conversely, the optimal phase velocity β_p of travelling wave corresponding to different incident velocities β_0 can be obtained in this way. Through extensive analysis of experimental data, it is convincingly demonstrated that the optimal phase velocity β_p should be 0.01 larger than the particle velocity β_0 to achieve maximum energy gain throughout the entire acceleration process.

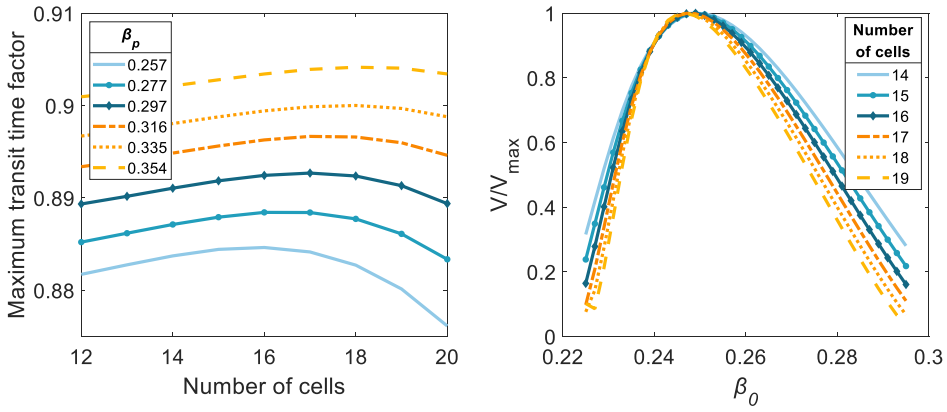

Fig.8 (color online) The maximum *TTF* varies with the Number of cells and phase velocity β_p (left)

V/V_{max} varies with the Number of cells and β_0, holding β_p constant (right)

The electric field on the axis of cavity and the optimal cavity geometric dimension are calculated by CST. The frequency, denoted as *f*, was adjusted by modifying the outer radius of the cell cavity, R_{out}, while maintaining a constant ratio of tube length (L_{tube}) to cell length (L_{cell}) at 0.6. And ensured that *f* remained at 2.856 GHz. Subsequently, the *PDT* code was utilized to calculate the optimal incident phase and energy gain as the particles passed through a 17-cell tank. The obtained parameters, such as the velocity β_p, cell length L_{cell}, and cavity nose length L_{tube}, were then used as inputs for CST in the next iteration. This iterative process was automated and repeated until the particle energy reached 100 MeV.

At the conclusion of the structure tuning simulation, the particle energy was accelerated to approximately 102.7 MeV. The specific parameters of the accelerating cavity can be found in Table 2.

Table 2 The specific parameters in each tank

Tank	Particle initial velocity β_0	Phase velocity β_p	Output energy [MeV]	Transit time factor (*TTF*)	Cell length [mm]
1	0.2470	0.2570	35.2910	0.884	11.8994
2	0.2668	0.2768	41.0496	0.889	12.8290
3	0.2865	0.2965	47.2542	0.894	13.7481
4	0.3059	0.3159	53.8974	0.898	14.6554
5	0.3251	0.3351	60.9820	0.902	15.5495
6	0.3440	0.3540	68.5051	0.906	16.4290
7	0.3626	0.3726	76.4541	0.909	17.2937
8	0.3808	0.3908	84.8124	0.912	18.1417
9	0.3987	0.4087	93.5835	0.914	18.9721
10	0.4161	0.4261	102.7443	0.917	19.7841

The optimal incident phase is obtained through the optimization algorithm in *PDT* code. The *TTF* of particles in each tank is above 0.88, which achieves the desired acceleration efficiency. The total length of BTW structure is 2.708 m, which is designed for the main acceleration cavity.

4.2 Beam Matching

As far as the transverse divergency of the beam is concerned, the magnetic-quadrupole lenses are incorporated in. According to the design of the main acceleration section, the structure of the acceleration cavity is determined. *PDT* code is used to solve the magnetic field gradient of two quadrupole lenses with thickness of l=0.03m in the first lattice, and Twiss parameters and the gradient is obtained G_1=G_2=384*T*/*m*. In order to facilitate the experimental control and engineering manufacturing of PMQs, the other eight lens are set to be exactly the same as in the first lattice. The transverse

ellipses can almost be matched after five complete FODO-like lattice configurations. Fig.10 shows the normalized phase-space ellipses at the beginning and the end of the linac and the envelope curves are successfully limited to an acceptable range.

The normalized emittance, as shown in Fig.9, remained at about 0.1 π·mm·mrad throughout the accelerating process, with a very small emittance growth rate and a complete beam transmission.

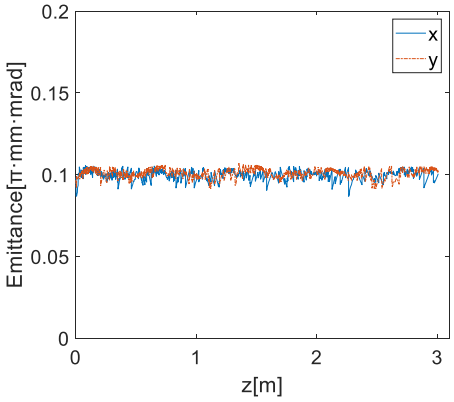

Fig.9 (color online) Normalized transverse emittance variation

Then the longitudinal multi-particle tracking simulation is carried out. The maximum longitudinal phase angle offset is assumed to be $\Delta\varphi = \pm 5°$and the initial maximum energy difference is $\Delta W = \pm 0.1 MeV$ relative to the incident reference particle. And ideally, the particles are evenly distributed in the longitudinal phase space. After the overall accelerating, the phase space envelope diagram of the longitudinal bunched beam is shown in Fig.10. It is found that the ellipse of particles within a certain range of the phase and energy from reference particle, when the acceleration period has terminated the phase width occupied by the bunched beam compresses in the longitudinal direction, while the energy spread increases.

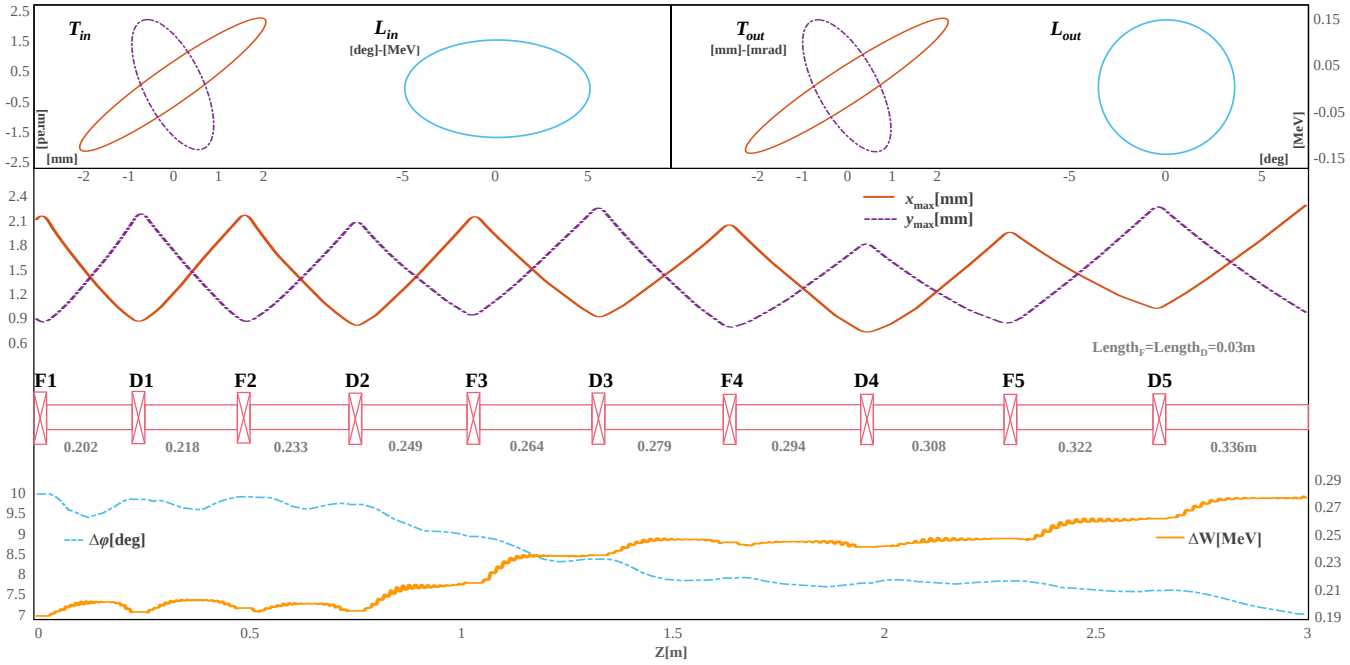

Fig.10 (color online) Configuration of the overall structure of linac (F and D are quadrupole lenses), with the envelope throughout the acceleration (x_{max}, y_{max}, Δφ and ΔW) and the normalized phase-space ellipses at the beginning and the end of the acceleration (*T* is transverse while *L* is longitude representing on the same axes respectively)

5 Conclusion

This paper presents the development of a new particle dynamics tracking (*PDT*) code that optimizes the dimensions of the overall accelerating structure and establishes electromagnetic fields in different acceleration tanks according to the particle motion with CST and MATLAB co-simulation. It supports both standing wave and travelling wave configurations, making it a versatile tool for a variety of particle types. Additionally, the code allows for the inclusion of additional elements, such as PMQs or solenoid for transverse beam focusing. And a benchmark is successfully performed.

The proposed high gradient proton linac, based on the BTW structure, is divided into 10 acceleration tanks with increasing length. Between the tanks, 10 PMQs are placed for transverse focusing of the bunched beam. The linac stretches a total length of approximately 3 m, and the overall configuration of the structure is depicted in Fig.10. The target average gradient for the BTW structure is 30 MV/m, and the overall average *TTF* of the acceleration cavity is 0.9, with the characteristics of full transmission and minimum emittance growth.

Acknowledgments

This work is supported by the National Natural Science Foundation of China (Grant Nos. 11375122 and 11875197). The authors would like to express their thanks to colleagues in the institute of modern physics for the cooperation on the electromagnetic calculation with CST.

References:

[1] WAN Xinmiao, PU Xuejiang, REN Zhiqiang *et al.* Discussion of 90° stopband in low-energy superconducting linear accelerators[J]. Nucl Sci Tech, 2022, 33(121):0-10. doi: 10.1007/s41365-022-01104-z

[2] FITZGERALD T J, BISHOP-JODOIN M. Proton Therapy - Current Status and Future Directions[M]. USA, IntechOpen, 2021. doi: 10.5772/intechopen.91072

[3] SAMY H. RF linear accelerators for medical and industrial Applications[M]. Boston/London, Artech House, 2012:1–10.

[4] Particle Therapy Cooperative Group (PTCOG) Collaboration. [2023-08-05]. http://www.ptcog.com

[5] AMALDI U, BERRA P, CRANDALL K *et al.* LIBO—A linac booster for proton therapy: Construction and test of a prototype[J]. Nucl Inst Methods Phys Res A, 2004, 521(2-3): 516-529. doi: 10.1016/j.nima.2003.07.062

[6] AMALDI U, BONOMI R, BRACCINI S, *et al.* Accelerators for hadrontherapy: From Lawrence cyclotrons to linacs[J]. Nucl Inst Methods Phys Res A, 2010, 620(2-3): 563-577. doi: 10.1016/j.nima.2010.03.130

[7] FAILLACE L, AGUSTSSON R, FRIGOLA P, *et al.* Fabrication and initial tests of an ultra-high gradient compact s-band (HGS) accelerating structure*[C]. Proceedings of the 3rd International Particle Accelerator Conference (IPAC-2012), New Orleans, Louisiana, 2012: 20-25.

[8] KUTSAEV S V, AGUSTSSON R, FAILLACE L, *et al.* High Gradient Accelerating Structures for Carbon Therapy Linac[C]. Proceedings of the 28th Linear Accelerator Conference (LINAC 16), East Lansing, September 2016.

[9] KUTSAEV S V. High-gradient low-β accelerating structure using the first negative spatial harmonic of the fundamental mode[J]. Phys Rev Accel Beams, 2017, 20(120401):0-16. doi: 10.1103/PhysRevAccelBeams.20.120401

[10] TraceWin. [2023-08-05]. http://irfu.cea.fr/dacm/en/logiciels

[11] ZHANG Yu, FANG Wencheng, HUANG Xiaoxia, *et al.* Design, fabrication, and cold test of an S-band high-gradient accelerating structure for compact proton therapy facility[J]. Nucl Sci Tech,2021,32(4):0-10. doi: 10.1007/S41365-021-00869-Z

[12] HUANG Xiaoxia, FANG Wencheng, GU Qiang *et al.* Design of an X-band accelerating structure using a newly developed structural optimization procedure[J]. Nucl Inst Methods Phys Res A,2017, 834(2017): 45–52. doi: 10.1016/j.nima.2017.02.050

[13] BENEDETTI S, AMALDI U, GRUDIEV A *et al.* Design of a Proton Travelling Wave Linac with a Novel Tracking Code[C]. Proceedings of the 6th International Particle Accelerator Conference (IPAC 2015), Richmond, VA, USA, May 2015.

[14] LATINA A. RF-Track Reference Manual (draft)[M]. Switzerland, 2020. doi: 10.5281/zenodo.3887085

[15] BILLEN J H, YOUNG L M. Poisson Superfish[M]. 2006.

[16] CST STUDIO SUITE. [2023-08-05]. https://www.cst.com/

[17] ZIEMANN V, Hands-On Accelerator Physics Using MATLAB[M]. CRC Press, Boca Raton, 2019. doi: 10.1201/9780429491290

[18] DONG Ye, DONG Zhiwei, ZHOU Haijing. A New Numerical Method for Solving Dispersion Curves of slow-wave Structures[J]. Information and Electronic Engineering, 2006, 2006(05): 331-336(in Chinese).

[19] LOEW G, MILLER R. Computer Calculations of Traveling-Wave Periodic Structure Properties[J]. IEEE T Nucl Sci,1979, 26(03):3701-3704. doi: 10.1109/TNS.1979.4330585

[20] LAPOSTOLLE P M, SEPTIER A L. Linear Accelerators[M]. North-Holland Pub. Co., France, 1970: 60-64.

[21] WANGLER T P. RF Linear Accelerators[M]. Wiley-VCH, Berlin, 2008. doi: 10.1002/9783527623426

[22] LIU Ning. Preparation of radioactive isotopes by CS-30 cyclotron and their application[J]. J Isotopes, 2012, 25(3): 189-192.

[23] LI Haoyun, Wan Xinmiao, CHEN Wei *et al*. Optimization of the S-band side-coupled cavities for proton acceleration[J]. Nucl Sci Tech, 2020, 31(02): 343-362. doi: 10.1007/s41365-020-0735-7

[24] BENEDETTI S, GRUDIEV A, LATINA A. High gradient linac for proton therapy[J]. Phys Rev Accel Beams,2017, 20(4):0-18. doi: 10.1103/PhysRevAccelBeams.20.040101

[25] BENEDETTI S, GRUDIEV A, LATINA A *et al*. RF Design of a Novel S-Band Backward Traveling Wave Linac for Proton Therapy[C]. Proceedings of the 27th Linear Accelerator Conference (LINAC 14), Switzerland, September 2014.

质子行波直线加速器的束流动力学模拟程序设计

杨玥菲，万鑫淼，蒲雪江，任志强，林鹏太，李智慧†

（辐射物理及技术教育部重点实验室，原子核科学技术研究所，四川大学；成都 610065）

摘要： 荷能质子束在癌症治疗、工业发展和科学研究等方面的广泛应用，使得质子加速器的研究日益升温。近年来，数 GHz 的高梯度射频驻波和行波结构的发展为紧凑型粒子直线加速器的研究提供了新的思路。然而，与丰富的驻波粒子直线加速器设计工具相比，行波直线加速器的仿真设计工具非常有限。因此开发了一个基于行波结构的粒子动力学跟踪（PDT）程序来模拟粒子的状态轨迹，同时满足对整体加速链各个元件的自动调谐。其模块化结构使其可以根据仿真设计需求调整添加功能，包括对类 FODO 结构束流匹配以及寻求能量调制需要的最优起点等。与 TraceWin 直线束流动力学仿真程序进行了比较测试，结果表明该方法在能量增益和束流匹配上都具有良好的精度。该程序已应用于一个工作频率为 2.856 GHz 的低流强返行波质子直线加速器的束流动力学设计中。该直线加速器全长约 3 米，由 10 个加速段和 10 个四极永磁磁铁组成，加速梯度为 30 MV/m，具有完全传输和低发射度增长的特点。

关键词： 质子束；行波；粒子动力学；束流匹配；直线加速器

收稿日期： yyyy-mm-dd; **修改日期：** yyyy-mm-dd

基金项目： 国家自然科学基金资助项目(11375122, 11875197)

通信作者： 李智慧，E-mail: lizhihui@scu.edu.cn